2.2. FORCED DYNAMICS CONTROL OF INDUCTION MOTOR WITH SELECTABLE FORCED DYNAMICS

Abstract: This section describes a further development of the FDC control system for IM drives presented in section 2.1, in which the prescribed response to the reference speed demand can be chosen according to the constant acceleration, constant jerk, linear first order and linear second order dynamic modes, described in Chapter 1. The control system, as developed to date, would be suited very well to applications requiring control to a moderate accuracy. Experimental results obtained indicate good agreement with the theoretical predictions.

2.2.1 Introduction

A new approach is taken to the control of induction motor based electric drives without the aid of shaft mounted speed or position sensors. The result is a control law, which may be operated in any one of the operating modes described in Chapter 1.

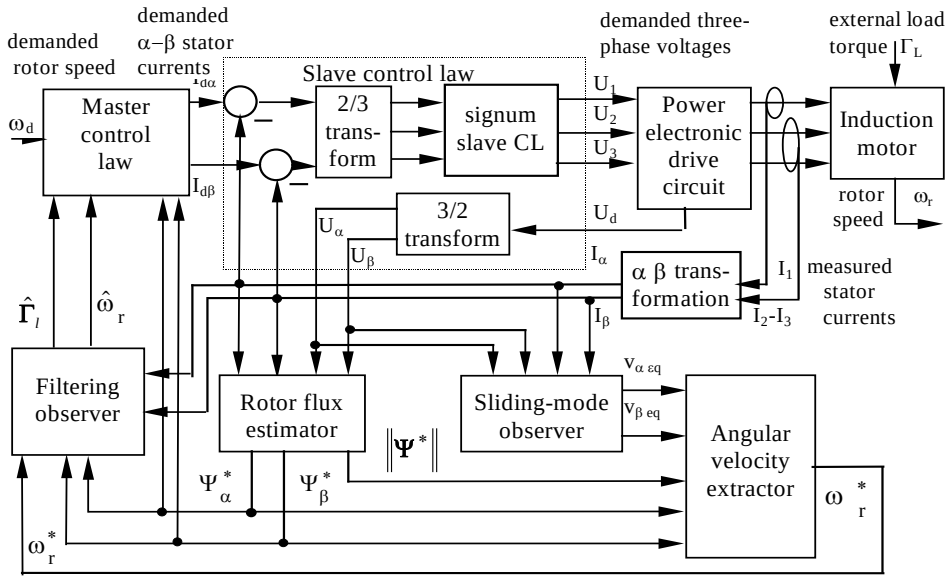

Fig. 2.2.1 Overall control system block diagram

The drive control system has a cascaded loop structure, as shown in Fig. 2.2.1, comprising an inner current control loop and an outer control loop realising the closed-loop dynamic behaviour of the selected operational mode. The inner control loop forces the three-phase stator currents to follow their demands with negligible dynamic lag by setting the switching state of the three-phase inverter to oppose the errors between the demanded and measured stator currents at every iteration interval.

Since the only measurement variables are the stator currents, a rotor speed estimator is employed which requires just these measurements together with the known stator voltages and estimated magnetic flux components from a magnetic flux estimator. An observer whose real time model is based on the motor mechanical equation produces a load torque estimate required by the outer loop control law. This requires the output of the speed estimator, the measured stator current components, the known stator voltage components and estimated magnetic flux components as inputs.

2.2.2 The Control Law Development

In the interests of simplification, the control system is arranged in a hierarchical structure [1] in which the stator current demands are generated as primary control variables by a *master control law***,** to be followed closely by a *slave control law* using the true control variables, i.e., the stator voltages.

2a) Model of Induction Motor

The following non-linear differential equations formulated in the stator-fixed α, β co-ordinate system describe the induction machine and serve for development of the control system:

$$\dot{\mathbf{I}} = c_1\left[c_2\mathbf{P}(\omega_r)\boldsymbol{\Psi} - a_1\mathbf{I} + \mathbf{U}\right] \tag{2.2.1}$$

$$\dot{\boldsymbol{\Psi}} = -\mathbf{P}(\omega_r)\boldsymbol{\Psi} + c_4\mathbf{I} \tag{2.2.2}$$

$$\dot{\omega}_r = \frac{1}{J}(\Gamma - \Gamma_L) = \frac{1}{J}\left(c_5\boldsymbol{\Psi}^T\mathbf{T}^T\mathbf{I} - \Gamma_L\right), \tag{2.2.3}$$

where $\boldsymbol{\Psi}^T = \begin{bmatrix} \Psi_\alpha & \Psi_\beta \end{bmatrix}$ is the rotor magnetic flux, $\mathbf{I}^T = \begin{bmatrix} i_\alpha & i_\beta \end{bmatrix}$ is the stator current, $\mathbf{U}^T = \begin{bmatrix} u_\alpha & u_\beta \end{bmatrix}$ is the stator voltage, $\boldsymbol{\Gamma}$ is the torque developed by the motor, ω_r is the mechanical rotor speed, $c_i, i = 1,2,3,4,5$ and a_1 are constants, given by: $c_1 = L_r / \left(L_s L_r - L_m^2\right)$, $c_2 = L_m / L_r$, $c_3 = R_r / L_r = 1/T_r$, $c_4 = L_m / T_r$, $c_5 = 3pL_m / 2L_r$, $a_1 = R_s + \left(L_m^2 / L_r^2\right) R_r$, where L_s, L_r and L_m are, respectively, the stator and rotor inductances and the mutual inductance between the rotor and the stator. R_s and R_r are, respectively, the stator and rotor resistances and p is the number of stator pole pairs. Also

$$\mathbf{P}\left(\omega_r\right) = \begin{bmatrix} c_3 & p\omega_r \\ -p\omega_r & c_3 \end{bmatrix} \quad \text{and} \quad \mathbf{T} = \begin{bmatrix} 0 & -1 \\ 1 & 0 \end{bmatrix}. \tag{2.2.4}$$

2b) The Master Control Law

The feedback linearisation principles [2] are used for the control law development. The *linearising functions* which force the system variables to obey specified closed-loop differential equations are formulated for the rotor speed and the magnetic flux norm. Firstly they are assumed linear, first order with time constant T_ω for rotor speed and with time constant T_ψ for demanded rotor flux norm. These two variables therefore satisfy:

$$\dot{\omega}_r = \frac{1}{T_\omega}\left(\omega_d - \omega_r\right) = a_d \tag{2.2.5a}$$

$$\left\|\dot{\Psi}\right\| = \frac{1}{T_\Psi}\left(\left\|\Psi\right\|_d - \left\|\Psi\right\|\right). \tag{2.2.5b}$$

The linearising function for $\dot{\omega}_r$ is obtained simply by equating the right hand sides of equations (2.2.3) and (2.2.5a), as follows:

$$\boldsymbol{\Psi}^T \mathbf{T}^T \mathbf{I} = \frac{1}{c_5}\left[\frac{J}{T_\omega}\left(\omega_d - \omega_r\right) + \boldsymbol{\Gamma}_L\right] \tag{2.2.6}$$

$$\boldsymbol{\Psi}^T \mathbf{T}^T \mathbf{I} = \frac{1}{c_5}\left[J \cdot a_d + \Gamma_L\right]. \tag{2.2.7}$$

The rotor magnetic flux norm $\|\Psi\|$ is defined by equation (2.2.8) and its derivative $\|\dot{\Psi}\|$ can be shown to be given by equation (2.2.9):

$$\|\Psi\|(t) = \Psi_\alpha^2 + \Psi_\beta^2 \tag{2.2.8}$$

$$\|\dot{\Psi}\| = -2\left(c_3\|\Psi\| - c_4 \boldsymbol{\Psi}^T * \mathbf{I}\right). \tag{2.2.9}$$

Again by equating the right hand sides of equations (2.2.5b) and (2.2.9) for the rotor flux norm derivative yields:

$$\boldsymbol{\Psi}^T\mathbf{I} = \frac{c_3}{c_4}\|\Psi\| + \frac{1}{2c_4T_\Psi}\left(\|\Psi\|_d - \|\Psi\|\right). \tag{2.2.10}$$

The required control law is then obtained by combining equations (2.2.6) and (2.2.10). But before this is done, the state variables (x) are replaced by their estimates, $(\hat{x})$ from the observers. Also, the constant motor parameters (p) are replaced by estimates $(\tilde{p})$ as they cannot be known with infinite precision in practice. Furthermore, the fictitious control vector, **I**, is replaced by the demanded current vector, $\mathbf{I_d}$, which will form the reference input to the slave control law to be described subsequently. Thus:

$$\mathbf{I}_d = \frac{1}{\|\hat{\Psi}\|}\begin{bmatrix} -\hat{\Psi}_\beta & \hat{\Psi}_\alpha \\ \hat{\Psi}_\alpha & \hat{\Psi}_\beta \end{bmatrix}\begin{bmatrix} \frac{1}{\tilde{c}_5}\left[\frac{\tilde{J}}{T_\omega}\left(\omega_d - \hat{\omega}_r\right) + \hat{\Gamma}_L\right] \\ \frac{\tilde{c}_3}{\tilde{c}_4}\|\hat{\Psi}\| + \frac{1}{2\tilde{c}_4T_\Psi}\left(\|\Psi\|_d - \|\hat{\Psi}\|\right) \end{bmatrix} \tag{2.2.11}$$

$$\mathbf{I}_d = \frac{1}{\|\hat{\Psi}\|}\begin{bmatrix} -\hat{\Psi}_\beta & \hat{\Psi}_\alpha \\ \hat{\Psi}_\alpha & \hat{\Psi}_\beta \end{bmatrix}\begin{bmatrix} \frac{1}{\tilde{c}_5}\left[\Gamma_{dyn} + \hat{\Gamma}_L\right] \\ F(\Psi) \end{bmatrix}, \tag{2.2.12}$$

where:

$$F(\Psi) = \frac{\tilde{c}_3}{\tilde{c}_4}\|\hat{\Psi}\| + \frac{1}{2\tilde{c}_4T_\Psi}\left(\|\Psi\|_d - \|\hat{\Psi}\|\right) \tag{2.2.13}$$

$$\Gamma_{dyn} = \tilde{J}\cdot a_d \qquad \text{and} \qquad a_d = \left[\frac{1}{T_\omega}\left(\omega_d - \hat{\omega}_r\right)\right]. \tag{2.2.14}$$

The control algorithm (2.2.11) contains the demanded output shaft angular acceleration a_d (2.2.14). The three following operational modes are realised by means of three differential equations for the angular acceleration, a_d. The example of equation (2.2.14) yields the first order dynamics referred to below. The second part (2.2.13) of the control law is the same for all three modes and is merely a statement of the prescribed rotor flux dynamics.

2b1) The acceleration and dynamic torque for direct acceleration control

In this case, the demanded acceleration is determined by a constant demanded angular velocity, ω_d , and a demanded acceleration time, $T_s=T_{ramp}$:

$$a_d = \frac{\omega_d}{T_s}\,\mathrm{sgn}\left(\omega_d - \hat{\omega}_r\right). \tag{2.2.15}$$

2b2) The acceleration and dynamic torque for linearly changing acceleration

For this operational mode, the value of the acceleration derivative '**ε**' during speed-up is constant and the maximum acceleration is achieved in the middle of this interval. For these values and for demanded acceleration and dynamic torque is therefore valid:

$$\varepsilon = \frac{4}{T_s^2}\omega_d \qquad (2.2.16) \qquad\qquad a_{max} = \frac{2}{T_s}\omega_d \qquad (2.2.17)$$

$$\begin{aligned} a_d &= \varepsilon t \cdot \mathrm{sgn}\left(\omega_d - \hat{\omega}_r\right) && \text{for} \quad t \in \left(0, \frac{T_s}{2}\right); \\ a_d &= \varepsilon T_s\left(1 - \frac{t}{T_s}\right)\cdot \mathrm{sgn}\left(\omega_d - \hat{\omega}_r\right) && \text{for} \quad t \in \left(\frac{T_s}{2}, T_s\right). \end{aligned} \tag{2.2.18}$$

2b3) The acceleration and dynamic torque for first order dynamics

This case was already described during master control law development. Thus:

$$a_d = \frac{3}{T_s}\left(\omega_d - \omega_r\right). \tag{2.2.19}$$

2b4) The acceleration and dynamic torque for second order dynamics

In this case, the desired closed-loop differential equation for the ideal rotor speed is done by (2.2.20). If the poles of this equation are purposely chosen as coincident and damping factor ξ=1, the settling time formula done by (2.2.21) may be used to determine ω_{nat} (where '*n*' is order of the system) to fit chosen settling time:

$$\ddot{\omega}_{id} = -2\xi\omega_{nat}\dot{\omega}_{id} + \omega_{nat}^2\left(\omega_{dem} - \omega_{id}\right) \tag{2.2.20}$$

$$T_s = 1.5 * (1+n)\frac{1}{\omega_{nat}}. \tag{2.2.21}$$

If equation (2.2.20) is numerically integrated then $\dot{\omega}$ is the demanded angular acceleration:

$$a_d(k+1) = a_d(k) + \left[\omega_{nat}^2\left(\omega_{dem} - \hat{\omega}_r\right) - 2\xi\omega_{nat}a_d(k)\right]\cdot h \tag{2.2.22}$$

Profiles of speed and acceleration for individual dynamics were shown in Fig. 1.3.1.

2.2.3 Estimation and Filtering

The Rotor Flux Estimator estimates the rotor magnetic flux vector components independently from the rotor angular velocity and is derived by first eliminating the term, $\mathbf{P}\left(\omega_r\right)\boldsymbol{\Psi}$, between equations (2.2.1) and (2.2.2) and then substituting this in equation (2.2.2), yielding:

$$\boldsymbol{\Psi} = \int\left[\left(c_4 - \frac{a_1}{c_2}\right)\mathbf{I} + \left(\frac{1}{c_2}\right)\mathbf{U}\right]dt - \left(\frac{1}{c_1 c_2}\right)\mathbf{I}. \tag{2.2.23}$$

This was implemented by simple explicit Euler numerical integration. The integration, however, would be subject to long-term drift in practice and special measures should be taken to correct for this. The correction for steady-state may

be done without distortion of the magnitudes and phases of the flux estimates relative to the real fluxes [3].

The Sliding Mode Observer and Angular Velocity Extractor are used to determine rotor speed. First, a stator current vector *pseudo sliding-mode* observer is formulated for generation of an unfiltered estimate, $\tilde{c}_1\tilde{c}_2\mathbf{P}(\omega_r^*)\boldsymbol{\Psi}^*$ of the term, $c_1c_2\mathbf{P}(\omega_r)\boldsymbol{\Psi}$, of equation (2.2.1), by means of the *equivalent control method* [4], from which will be extracted an unfiltered estimate, ω_r^* of ω_r, with the aid of the flux estimate, $\boldsymbol{\Psi}^*$, from the rotor flux estimator of the previous section.

The basic stator current vector sliding-mode observer is given by:

$$\dot{\mathbf{I}}^* = \tilde{c}_1\left[-\tilde{a}_1\mathbf{I}^* + \mathbf{U}\right] - \mathbf{v}\,, \tag{2.2.24}$$

where, $\mathbf{I}^*$ is an estimate of $\mathbf{I}$ as in a conventional observer. The required estimate, however, is not $\mathbf{I}^*$ but the continuous value of $\mathbf{v}$ which is generated by a *pseudo-sliding-mode* observer as:

$$\mathbf{v} = -\mathbf{K}_I\left[\mathbf{I} - \mathbf{I}^*\right], \tag{2.2.25}$$

where $\mathbf{K}_I$ is diagonal matrix with elements, k_i, so that $\mathbf{v}$ is continuous. Then assuming that $\mathbf{I}^* = \mathbf{I}$, and replacing $\boldsymbol{\Psi}$ and ω_r in equation (2.2.1), respectively, by their estimates, $\boldsymbol{\Psi}^*$ and ω_r^*:

$$\mathbf{v}_{eq}^* = -\tilde{c}_1\tilde{c}_2\mathbf{P}(\omega_r^*)\boldsymbol{\Psi}^*. \tag{2.2.26}$$

Estimate of rotor speed, ω_r^* is then extracted by subtracting the component equations of (2.2.26) to yield:

$$\omega_r^* = \left[\mathbf{v}_{eq}^*\right]^T\mathbf{T}\boldsymbol{\Psi}^* \Big/ \left(\tilde{c}_1\tilde{c}_2 p\|\boldsymbol{\Psi}^*\|\right). \tag{2.2.27}$$

The Filtering Observer presented previously caters for plant and measurement of noise, producing a filtered angular velocity estimate, $\hat{\omega}_r$. Finally, since there is no direct means of measuring the external load torque, Γ_L, is treated as a state variable in the real time model of the observer and is thereby estimated.

The filtering observer is as follows:

$$\begin{aligned} e_\omega &= \omega_r^* - \hat{\omega} \\ \dot{\hat{\omega}}_r &= \frac{1}{\tilde{J}}\left(\tilde{c}_5 \left[\boldsymbol{\Psi}^*\right]^T \mathbf{T}^T \mathbf{I} - \hat{\Gamma}_L \right) + k_\omega e_\omega \,. \\ \dot{\hat{\Gamma}}_L &= k_\Gamma e_\omega \end{aligned} \tag{2.2.28}$$

This is a conventional second order linear observer with a correction loop characteristic polynomial, which may be chosen via gains k_ω and k_Γ, to yield desired balance of filtering between the noise from measurements of currents i_α and i_β and the noise from velocity estimate (*measurements*) ω_r^*. With respect of settling time formula (2.2.21), for n=2, $T_s = 9/(2\omega_n)$ the observer poles can be design as:

$$s^2 + 2\omega_n s + \omega_n^2 = s^2 + s k_\omega + \frac{k_\Gamma}{J} \tag{2.2.29a}$$

$$k_\omega = \frac{9}{T_s} \quad a \qquad k_\Gamma = \frac{81J}{4T_s^2} \,. \tag{2.2.29b}$$

A modified version of the observer based on pole placement at two different locations, $-\omega_1$ and $-\omega_2$, which shows higher stability, was used for design of observer gains k_ω and k_Γ. Thus:

$$s^2 + s(\omega_1 + \omega_2) + \omega_1\omega_2 = s^2 + s k_\omega + \frac{k_\Gamma}{J}, \tag{2.2.30a}$$

$$k_\omega = (\omega_1 + \omega_2) \quad \text{and} \qquad k_\Gamma = J \cdot \omega_1 \cdot \omega_2 \,. \tag{2.2.30b}$$

2.2.4 Experimental Results

The parameters of the IM and ancillary devices used for experiments are listed in the Appendix. IM was equipped by eddy-current brake. The control law was implemented via a Pentium PC166, the stator currents being measured through LEM transformers and evaluated using a PC Lab Card PCL812 built direct into the

PC. An IGBT transistor module FUJI 2803 6MBI10L-060 was used as a three-phase inverter, when the dc bus voltage was equal U_{dc}=52.5 V.

The experiments for all three prescribed dynamics were carried out for the same speed demand ω_d = 200 rad/s with settling time T_s = 1 s. Magnetic flux norm demand was kept constant and equal to $\|\Psi\|_d$ = 0,0025 $(Vs)^2$ with time constant T_Ψ = 3 ms.

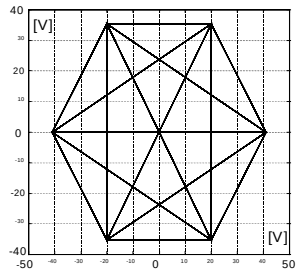

a) Complex stator voltages $u_\alpha=f(u_\beta)$

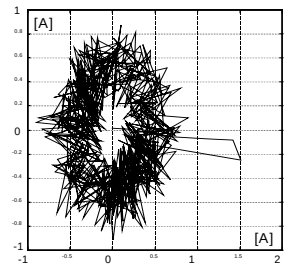

b) Complex stator currents $i_\alpha=f(i_\beta)$

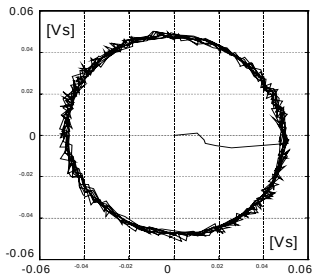

c) Complex rotor fluxes $\Psi_\alpha=f(\Psi_\beta)$

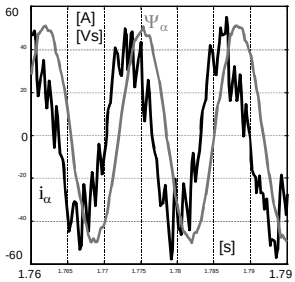

d) Steady-state current and rotor flux v. time

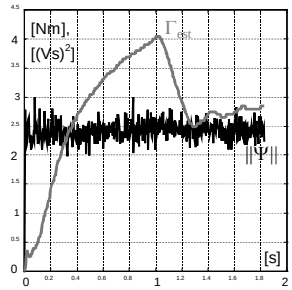

e) Estimated magnetic flux norm and torque v. time

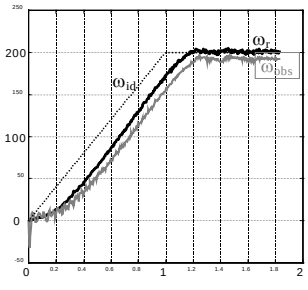

f) Ideal speed, rotor speed and estimated speed v. t.

Fig. 2.2.2 Experimental results for IM in constant torque acceleration mode

All presented figures contain (a) complex stator voltages, (b) complex stator currents, and (c) complex rotor magnetic flux. Steady state α-

components of stator currents, (*multiplied by 1e2*), and rotor flux (*multiplied by 1e3*) as a function of time are shown in (d) for time interval t = 1,78-1,79 s. Estimated rotor flux norm and load torque estimate are shown in (e) and finally subplot (f) shows ideal speed response, real rotor speed and its estimate from filtering observer.

Experimental results for IM and direct acceleration control are shown in Fig. 2.2.2. The range of rotor speeds achieved is ω_d = 20-250 rad/s with prescribed time constants T_ω = 0,05-1 s. It can be clearly seen from Fig. 2.2.2 that ramp increase of speed was achieved with short delay.

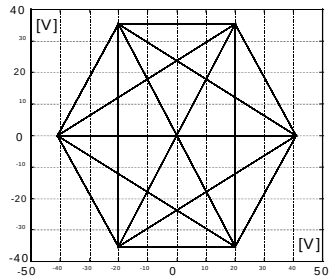

a) Complex stator voltages u_α=f(u_β)

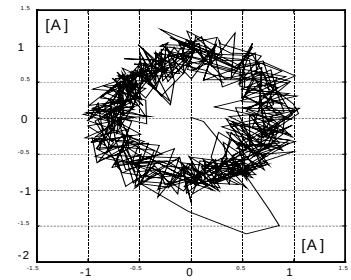

b) Complex stator currents i_α=f(i_β)

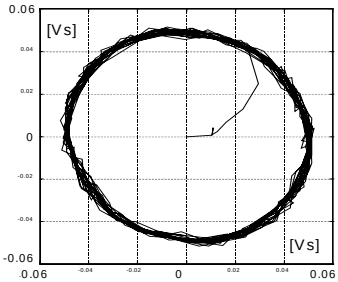

c*) Complex rotor fluxes* Ψ_α=f(Ψ_β)

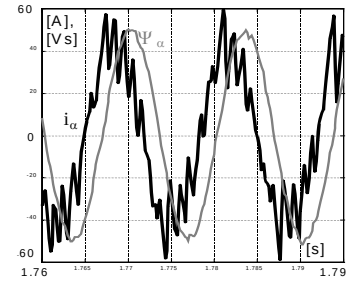

d) Steady-state stator current & rotor flux v. t.

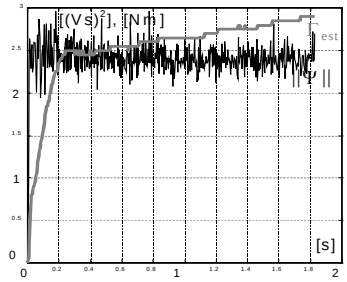

e) Estimated magnetic flux norm and torque v. t.

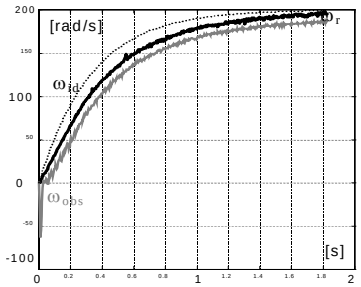

f) Ideal speed, rotor speed and estimated speed v. t.

torque v. t.

Fig. 2.2.3 Experimental results for IM with first order dynamics

Experimental results for first order dynamics are shown in Fig. 2.2.3. The achieved control range of shaft angular speed is ω_d=15-250 rad/s with prescribed time constants T_ω=0,1-1 s. Again the demanded dynamics were achieved with short delays.

Experimental results for second order dynamics are shown in Fig. 2.2.4. The achieved control range is again ω_{dem}=15-250 rad/s with prescribed time constants T_ω=0,05-1 s. Again it can be clearly seen that demanded second order dynamic was achieved with small lag.

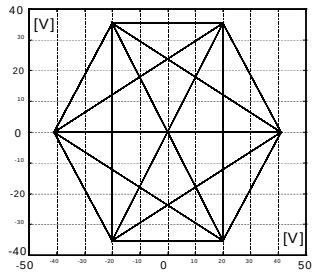

a) Complex stator voltages $u_\alpha=f(u_\beta)$

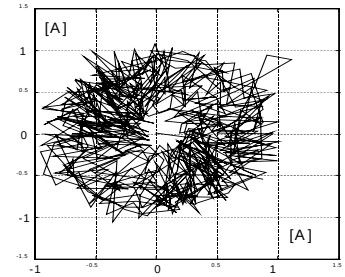

b) Complex stator currents $i_\alpha=f(i_\beta)$

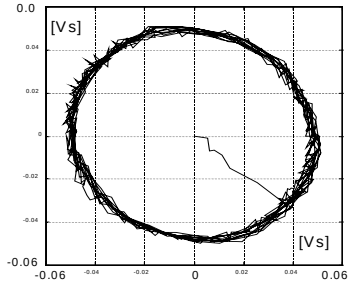

c) Complex rotor fluxes $\Psi_\alpha=f(\Psi_\beta)$

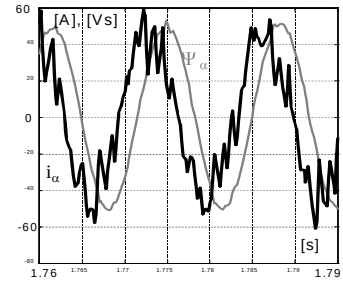

d) Steady-state current and rotor flux v. t.

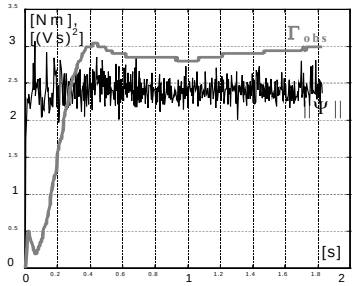

e) Estimated magnetic flux norm and

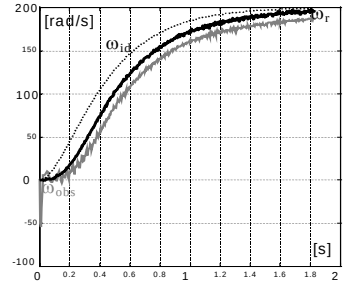

f) Ideal speed, rotor speed and estimated

torque v. t. *speed v. t.*

Fig. 2.2.4 Experimental results for IM with second order dynamics

Experimental results for the electric drive with IM and second order dynamics with various damping factor are shown in Fig. 2.2.5. It can be seen again that real rotor speed follows ideal speed response only with small lag for under-damped, ξ=0,5, critically damped, ξ=1and over-damped, ξ=1,5 system.

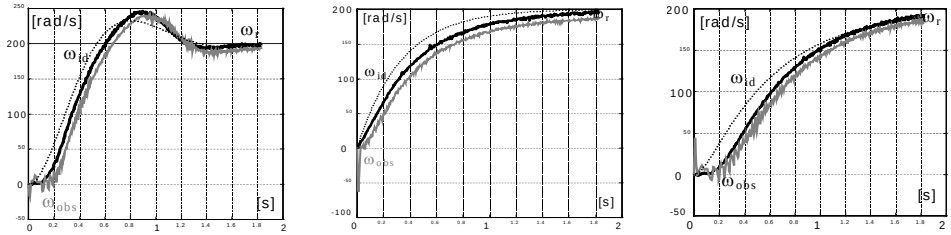

a) ξ = 0.5 b) ξ = 1.0 c) ξ = 1.5

Fig. 2.2.5 Experimental results for second order dynamics and various damping factor

Finally Fig.2.2.6 shows the experimental results for all four prescribed dynamics and idle running IM, when chosen speed reference was ω_{dem} = 200 rad/s and settling time T_s = 0,2 s and speed response is shown together with ideal one.

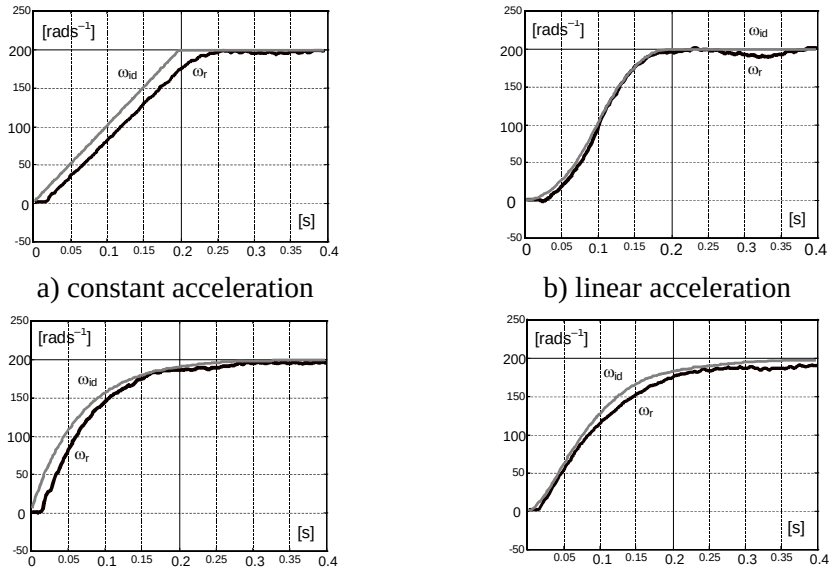

a) constant acceleration b) linear acceleration

c) first order dynamic d) second order dynamic

Fig. 2.2.6 Experimental results for IM with all individual dynamics

2.2.5 Conclusions

The investigations of the proposed new control method for electric drives employing induction motors with forced dynamics show a good agreement with the theoretical predictions. The significant, though not very large, departure from the ideal performance is due mainly to the non-zero iteration interval, h, and time delay in the load torque estimation as well as due to errors in the motor and load parameter estimation.

While direct torque control can be suitable for majority of industrial applications, second order dynamic can be very attractive for electric drive designers of cranes and lifts. The control system, as developed to date, would be suitable for applications requiring sensorless speed control of induction motor to moderate accuracy ($\approx 5\%$).

2.2.6 References

[1] UTKIN, V. A.: '*Method of separation of motions in observation problems*'. *Automation and Remote Control*, y. 1990, Vol. 44, No. 12, Part 1, pp. 300 - 308.

[2] ISIDORI, A.: '*Nonlinear Control Systems*' 2nd edition, *Springer-Verlag*, Berlin, 1990.

[3] DODDS, S. J., VITTEK, J.: '*An Algorithm for Magnetic Flux Computation with Automatic Drift Correction*'. Scientific Works and Studies of *University of Zilina*, Elektro S., Vol. 22, 1998, pp. 5 – 14.

[4] UTKIN, V. I.: '*Sliding Modes in Control and Optimisation'. Springer.Verlag*, Berlin, Heidelberg 1992.

[5] DODDS, S. J., VITTEK, J., ALEXÍK M.: '*Simulation of A New Control Law for Shaft Sensorless IM Drive with Prescribed Closed Loop Dynamics*'. *MOSIS'97*, Conf. Proceedings, Vol.3, Hradec nad Moravicí, Czech Republic, April 1997, pp. 236 – 243.

[6] DODDS, S. J., UTKIN, V. A., VITTEK, J.: *'Self Oscillating Synchronous Motor Drive Control System with Prescribed Closed-Loop Speed Dynamics*'. *2nd EPE Chapter Symposium* Proceedings, Vol. 2, Nancy, France, June 1996. pp. 23-28.

[7] DODDS, S. J., VITTEK, J., MIENKINA, M.: '*Implementation of a Sensorless Induction Motor Drive Control System with Prescribed Closed-Loop Rotor Magnetic Flux and Speed Dynamics*'. *EPE'97* European Conf. Proceedings, Trondheim, Norway, Sept. 1997, Vol. 4., pp. 4.492 - 4.497

[8] DODDS, S. J., VITTEK, J.: '*New Control Method for AC Motor Drives''*. *PEMC'98*, EPE Conf. Proceedings, Prague, Czech Republic, Sept. 1998, Vol. 5, pp. 5-173 - 5-178.

[9] VITTEK, J., ALTUS, J., DODDS, S., J., PERRYMAN, R.: '*Preliminary Experimental Results for Synchronous Motor Drive with Forced Dynamics*'. *IASTED'9*8, Conference Proceedings, Honolulu, HI, USA, August 1998, pp. 219-223.

Appendix

Three-phase e induction motor 4AP-64 P parameters are as follows:

Parameters of induction motor		**Equivalent circuit parameters**	
Rated power	P_n=180 W	Mutual inductance	L_m=1,083 H
Rated speed	n_n=1370 ot/min	Stator inductance	L_s=1,17 H
Rated current	I_n=1,15 A	Rotor inductance	L_r=1,17 H
Terminal voltage	U_n=220 V	Stator resistance	R_s=46,23 Ω
Moment of inertia	J=6,5e-4 kgm^2	Rotor resistance	R_r=15,39 Ω
Parameters of IGBT FUJI 6MBI-060		**Current sensors LEM**	
Rated voltage	600 V	LTA 50P/SPI	
Rated current	6x10 A		

Acknowledgements

The authors wish to thank to Daniel Vysoudil of the AD Developments Milton Keynes, United Kingdom for producing the experimental results for ‘Forced Dynamics Control’ and Ministry of Education, Slovak Republic, for funding the VEGA Project No.1/6111/99.